Journal of Innovative Optical Health Sciences
Vol. 9, No. 2 (2016) 1650021 (8 pages)

DOI: 10.1142/S1793545816500218

World Scientific
www.worldscientific.com

Image enhancement via MMSE estimation of Gaussian scale mixture with Maxwell density in AWGN

Pichid Kittisuwan
Department of Telecommunication Engineering
Faculty of Engineering
Rajamangala University of Technology (Ratanakosin)
Nakhonpathom, Thailand
pichidkit@yahoo.com; Pichid.Kit@rmutr.ac.th

Received 1 October 2015
Accepted 17 November 2015
Published 21 January 2016

In optical techniques, noise signal is a classical problem in medical image processing. Recently, there has been considerable interest in using the wavelet transform with Bayesian estimation as a powerful tool for recovering image from noisy data. In wavelet domain, if Bayesian estimator is used for denoising problem, the solution requires a prior knowledge about the distribution of wavelet coefficients. Indeed, wavelet coefficients might be better modeled by super Gaussian density. The super Gaussian density can be generated by Gaussian scale mixture (GSM). So, we present new minimum mean square error (MMSE) estimator for spherically-contoured GSM with Maxwell distribution in additive white Gaussian noise (AWGN). We compare our proposed method to current state-of-the-art method applied on standard test image and we quantify achieved performance improvement.

Keywords: Gaussian scale mixture; minimum mean square error estimation; image denoising; wavelet transforms.

1. Introduction

Image processing is the most popular technique used by doctors for the purpose diagnosis. In fact, noise signal reduction step is an essential part of many medical image processing applications, i.e., classification recognition and other application tasks.[1–3] Wavelet transform with Bayesian estimator has been proposed as a powerful tool for image denoising.[4] In fact, Bayesian methods require a prior distribution of wavelet coefficients and use minimum mean square error (MMSE) or maximum *a posteriori* (MAP) estimations to derive the mapping function (also known as shrinkage function) from noisy data to estimated data.[5] There are two major properties for wavelet coefficients[6–9]: (1) wavelet coefficients of noise-free data usually process peaked, zero-mean distributions, with heavier than Gaussian tails (also known as super Gaussian

density); (2) multivariate models (random vectors) offers advantages over univariate model, because dependencies between coefficients can be captured (also known as parent–child property). In fact, the super Gaussian random vectors can be generated by Gaussian scale mixture (GSM).[6,10–12] Various authors have proposed various GSM to approximate the distribution of wavelet coefficients. For example in Refs. 13 and 14, GSM with exponential density (also known as Laplace random vectors) and GSM with gamma density (also known as radial exponential or quasi-Laplace random vectors) are proposed to model the distribution of wavelet coefficients, respectively. However, no one uses GSM with Maxwell density for distribution of wavelet coefficients. In fact, Maxwell density is important one-side distribution in signal processing.[15,16] So, we derive new MMSE estimator for spherically-contoured GSM with Maxwell distribution in additive white Gaussian noise (AWGN). The proposed MMSE estimator is expressed in analytical form using the generalized incomplete gamma function. The description of this function can be found in Appendix A.

The remainder of this paper is organized as follows. Section 2, we present new MMSE estimation of GSM with Maxwell density in AWGN. Section 3, denoising results are compared with existing technique in both PSNR and visual qualities. The experimental results show that the proposed method yields good denoising results. Finally, the conclusion and discussion are given in Section 4.

2. MMSE of GSM with Maxwell Density in AWGN

In this section, we are interested in the problem of estimating d-component random vectors of noise-free wavelet coefficients, $\mathbf{X}$, in AWGN, $\mathbf{N}$,

$$\mathbf{Y} = \mathbf{X} + \mathbf{N},$$

where $\mathbf{Y}, \mathbf{X}, \mathbf{N} \in \mathbb{R}^d$. The estimation of $\mathbf{X}$ is based on observed random vectors $\mathbf{Y}$. In this work, random vectors $\mathbf{X}$ can be represented as spherically-contoured GSM

$$\mathbf{X} = A\mathbf{S},$$

where $\mathbf{S}$ is d-dimensional zero-mean Gaussian random vectors with variance σ^2, $f_{\mathbf{S}}(\mathbf{s}) = \frac{1}{(2\pi\sigma^2)^{d/2}} \exp\left(\frac{-\|\mathbf{s}\|^2}{2\sigma^2}\right)$, and A is Maxwell (scalar) random variable with parameters $K_1, K_2 > 0$,

$$f_A(a) = K_1 a^2 \exp(-K_2 a^2), \quad a > 0. \tag{1}$$

Using Jacobian transformation, the distribution of $\mathbf{X}$ is

$$f_{\mathbf{X}}(\mathbf{x}) = \int_0^\infty \frac{1}{a^d} f_A(a) f_{\mathbf{S}}(\mathbf{x}/a) da. \tag{2}$$

In the characteristic of noise, $\mathbf{N}$ is zero-mean Gaussian random vectors with noise variance σ_n^2,

$$f_{\mathbf{N}}(\mathbf{n}) = \frac{1}{(2\pi\sigma_n^2)^{d/2}} \exp\left(\frac{-\|\mathbf{n}\|^2}{2\sigma_n^2}\right).$$

The MMSE estimator of x_i given $\mathbf{Y}$ is given by[23]

$$\hat{x}_i = \frac{\int_{\mathbb{R}^d} x_i f_{\mathbf{X}}(\mathbf{x}) f_{\mathbf{N}}(\mathbf{y}-\mathbf{x}) d\mathbf{x}}{\int_{\mathbb{R}^d} f_{\mathbf{X}}(\mathbf{x}) f_{\mathbf{N}}(\mathbf{y}-\mathbf{x}) d\mathbf{x}}. \tag{3}$$

So, to develop (3) for MMSE estimator, it is often necessary to know the value of $\int_{\mathbb{R}^d} x_i f_{\mathbf{X}}(\mathbf{x}) f_{\mathbf{N}}(\mathbf{y}-\mathbf{x}) d\mathbf{x}$ and $\int_{\mathbb{R}^d} f_{\mathbf{X}}(\mathbf{x}) f_{\mathbf{N}}(\mathbf{y}-\mathbf{x}) d\mathbf{x}$.

Using (2), the value of $\int_{\mathbb{R}^d} f_{\mathbf{X}}(\mathbf{x}) f_{\mathbf{N}}(\mathbf{y}-\mathbf{x}) d\mathbf{x}$ becomes

$$\begin{aligned}
&\int_{\mathbb{R}^d} f_{\mathbf{X}}(\mathbf{x}) f_{\mathbf{N}}(\mathbf{y}-\mathbf{x}) d\mathbf{x} \\
&\quad = \int_{\mathbb{R}^d} \left[\int_0^\infty \frac{1}{a^d} f_A(a) f_{\mathbf{S}}(\mathbf{x}/a) da\right] f_{\mathbf{N}}(\mathbf{y}-\mathbf{x}) d\mathbf{x} \\
&\quad = \int_0^\infty f_A(a) \left[\int_{\mathbb{R}^d} \frac{1}{a^d} f_{\mathbf{S}}(\mathbf{x}/a) f_{\mathbf{N}}(\mathbf{y}-\mathbf{x}) d\mathbf{x}\right] da.
\end{aligned} \tag{4}$$

In Gaussian integration, the description can be found in Appendix B, using (1) and (B.1) in (4) gives

$$\begin{aligned}
&\int_{\mathbb{R}^d} f_{\mathbf{X}}(\mathbf{x}) f_{\mathbf{N}}(\mathbf{y}-\mathbf{x}) d\mathbf{x} \\
&\quad = \frac{K_1}{(2\pi)^{d/2}} \int_0^\infty \frac{a}{(a^2\sigma^2 + \sigma_n^2)^{\frac{d}{2}}} \\
&\qquad \times \exp\left(-K_2 a^2 - \frac{\|\mathbf{y}\|^2}{2(a^2\sigma^2 + \sigma_n^2)}\right) a da.
\end{aligned}$$

Changing the variable of integration, using $t = K_2\left(a^2 + \frac{\sigma_n^2}{\sigma^2}\right)$, gives

$$\begin{aligned}
&\int_{\mathbb{R}^d} f_{\mathbf{X}}(\mathbf{x}) f_{\mathbf{N}}(\mathbf{y}-\mathbf{x}) d\mathbf{x} \\
&\quad = \frac{K_1 K_2^{(d-3)/2}}{2(2\pi\sigma^2)^{d/2}} \exp\left(\frac{K_2\sigma_n^2}{\sigma^2}\right)
\end{aligned}$$

$$\times \int_{K_2\sigma_n^2/\sigma^2}^{\infty} \left(t - \frac{K_2\sigma_n^2}{\sigma^2}\right)^{1/2} t^{-d/2} \times \exp\left(-t - \frac{K_2\|\mathbf{y}\|^2}{2\sigma^2 t}\right) dt. \quad (5)$$

Using (2), the value of $\int_{\mathbb{R}^d} x_i f_{\mathbf{X}}(\mathbf{x}) f_{\mathbf{N}}(\mathbf{y}-\mathbf{x}) d\mathbf{x}$ becomes

$$\begin{aligned}\int_{\mathbb{R}^d} x_i f_{\mathbf{X}}(\mathbf{x}) f_{\mathbf{N}}(\mathbf{y}-\mathbf{x}) d\mathbf{x} &= \int_{\mathbb{R}^d} x_i \left[\int_0^{\infty} \frac{1}{a^d} f_A(a) f_{\mathbf{S}}(\mathbf{x}/a) da\right] f_{\mathbf{N}}(\mathbf{y}-\mathbf{x}) d\mathbf{x} \\ &= \int_0^{\infty} f_A(a) \left[\int_{R^d} \frac{x_i}{a^d} f_{\mathbf{S}}(\mathbf{x}/a) f_{\mathbf{N}}(\mathbf{y}-\mathbf{x}) d\mathbf{x}\right] da. \end{aligned} \quad (6)$$

Table 1. Average PSNR values of denoising images over ten runs for Barbara, Moon and Texture.

Standard deviation noise (σ_n)	10	15	20
Barbara			
MLAP-MMSE[13]	31.92	29.61	28.00
BayeShrink[20]	32.20	29.89	28.10
Proposed method	**32.34**	**30.00**	**28.47**
Moon			
MLAP-MMSE[13]	31.11	29.91	19.19
BayeShrink[20]	31.47	30.13	29.11
Proposed method	**31.95**	**30.38**	**29.22**
Cells			
MLAP-MMSE[13]	30.91	28.69	27.24
BayeShrink[20]	30.95	28.67	27.24
Proposed method	**31.00**	**28.93**	**27.59**

(a) (b) (c) (d)

Fig. 1. Comparison of denoising results of Barbara image with $\sigma_n = 10$: (a) Noise-free. (b) Noisy image. (c) MLAP-MMSE (PSNR = 31.92). (d) Proposed method (PSNR = 32.34).

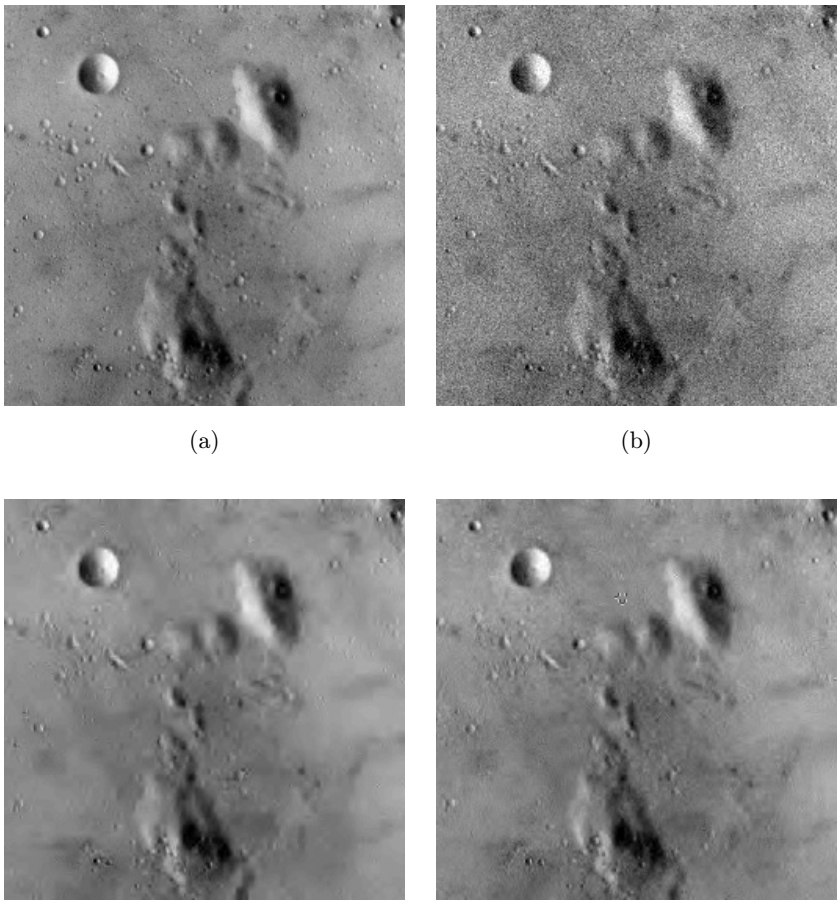

(a) (b)

(c) (d)

Fig. 2. Comparison of denoising results of Moon image with $\sigma_n = 15$: (a) Noise-free. (b) Noisy image. (c) MLAP-MMSE (PSNR = 29.91). (d) Proposed method (PSNR = 30.38).

In Gaussian integration, using (1) and (B.2) in (6) gives

$$\int_{\mathbb{R}^d} x_i f_{\mathbf{X}}(\mathbf{x}) f_{\mathbf{N}}(\mathbf{y}-\mathbf{x}) d\mathbf{x} = \frac{K_1 \sigma^2 y_i}{(2\pi)^{d/2}} \int_0^\infty \frac{a^3}{(a^2\sigma^2+\sigma_n^2)^{\frac{d}{2}+1}} \times \exp\left(-K_2 a^2 - \frac{\|\mathbf{y}\|^2}{2(a^2\sigma^2+\sigma_n^2)}\right) a da. \quad (7)$$

Changing the variable of integration, using $t = K_2(a^2 + \frac{\sigma_n^2}{\sigma^2})$, gives

$$\begin{aligned}\int_{\mathbb{R}^d} x_i f_{\mathbf{X}}(\mathbf{x}) f_{\mathbf{N}}(\mathbf{y}-\mathbf{x}) d\mathbf{x} &= \frac{K_1 K_2^{(d-3)/2}}{2(2\pi\sigma^2)^{d/2}} \exp\left(\frac{K_2\sigma_n^2}{\sigma^2}\right) y_i \\ &\quad \times \int_{K_2\sigma_n^2/\sigma^2}^\infty \left(t - \frac{K_2\sigma_n^2}{\sigma^2}\right)^{3/2} \\ &\quad \times t^{\frac{-d}{2}-1} \exp\left(-t - \frac{K_2\|\mathbf{y}\|^2}{2\sigma^2 t}\right) dt \\ &= \frac{K_1 K_2^{(d-3)/2}}{2(2\pi\sigma^2)^{d/2}} \exp\left(\frac{K_2\sigma_n^2}{\sigma^2}\right) y_i \\ &\quad \times \int_{K_2\sigma_n^2/\sigma^2}^\infty \left(t - \frac{K_2\sigma_n^2}{\sigma^2}\right)^{1/2} \\ &\quad \times \left(t - \frac{K_2\sigma_n^2}{\sigma^2}\right) t^{\frac{-d}{2}-1} \exp\left(-t - \frac{K_2\|\mathbf{y}\|^2}{2\sigma^2 t}\right) dt \\ &= \frac{K_1 K_2^{(d-3)/2}}{2(2\pi\sigma^2)^{d/2}} \exp\left(\frac{K_2\sigma_n^2}{\sigma^2}\right) y_i\end{aligned}$$

$$\times \left[\int_{K_2\sigma_n^2/\sigma^2}^{\infty} \left(t - \frac{K_2\sigma_n^2}{\sigma^2}\right)^{1/2} \times t^{\frac{-d}{2}} \exp\left(-t - \frac{K_2\|\mathbf{y}\|^2}{2\sigma^2 t}\right) dt - \left(\frac{K_2\sigma_n^2}{\sigma^2}\right) \times \int_{K_2\sigma_n^2/\sigma^2}^{\infty} \left(t - \frac{K_2\sigma_n^2}{\sigma^2}\right)^{1/2} t^{\frac{-d}{2}-1} \times \exp\left(-t - \frac{K_2\|\mathbf{y}\|^2}{2\sigma^2 t}\right) dt\right]. \quad (8)$$

Using (5) and (8) in (3) gives

$$x_i = y_i\left[1 - \left(\frac{K_2\sigma_n^2}{\sigma^2}\right) \times \frac{\int_{K_2\sigma_n^2/\sigma^2}^{\infty} \left(t - \frac{K_2\sigma_n^2}{\sigma^2}\right)^{1/2} t^{\frac{-d}{2}-1} \exp\left(-t - \frac{K_2\|\mathbf{y}\|^2}{2\sigma^2 t}\right) dt}{\int_{K_2\sigma_n^2/\sigma^2}^{\infty} \left(t - \frac{K_2\sigma_n^2}{\sigma^2}\right)^{1/2} t^{\frac{-d}{2}} \exp\left(-t - \frac{K_2\|\mathbf{y}\|^2}{2\sigma^2 t}\right) dt}\right]. \quad (9)$$

The approximation of square root function[19] is

$$\sqrt{a^2 + b} = a + \frac{b}{2a} - \frac{b^2}{8a^3} + \cdots. \quad (10)$$

So,

$$\left(t - \frac{K_2\sigma_n^2}{\sigma^2}\right)^{1/2} \approx t^{1/2} - \frac{K_2\sigma_n^2}{2\sigma^2 t^{1/2}}. \quad (11)$$

Using (11) and (A.1) in (9) gives

$$x_i = y_i\left[1 - \left(\frac{K_2\sigma_n^2}{\sigma^2}\right) \times \frac{\Gamma\left(\frac{-d}{2} + \frac{1}{2}, \frac{K_2\sigma_n^2}{\sigma^2}; \frac{K_2\|\mathbf{y}\|^2}{2\sigma^2}\right) - \frac{K_2\sigma_n^2}{2\sigma^2}\Gamma\left(\frac{-d}{2} - \frac{1}{2}, \frac{K_2\sigma_n^2}{\sigma^2}; \frac{K_2\|\mathbf{y}\|^2}{2\sigma^2}\right)}{\Gamma\left(\frac{-d}{2} + \frac{3}{2}, \frac{K_2\sigma_n^2}{\sigma^2}; \frac{K_2\|\mathbf{y}\|^2}{2\sigma^2}\right) - \frac{K_2\sigma_n^2}{2\sigma^2}\Gamma\left(\frac{-d}{2} + \frac{1}{2}, \frac{K_2\sigma_n^2}{\sigma^2}; \frac{K_2\|\mathbf{y}\|^2}{2\sigma^2}\right)}\right]. \quad (12)$$

Here, the proposed method is based on generalized incomplete gamma function.

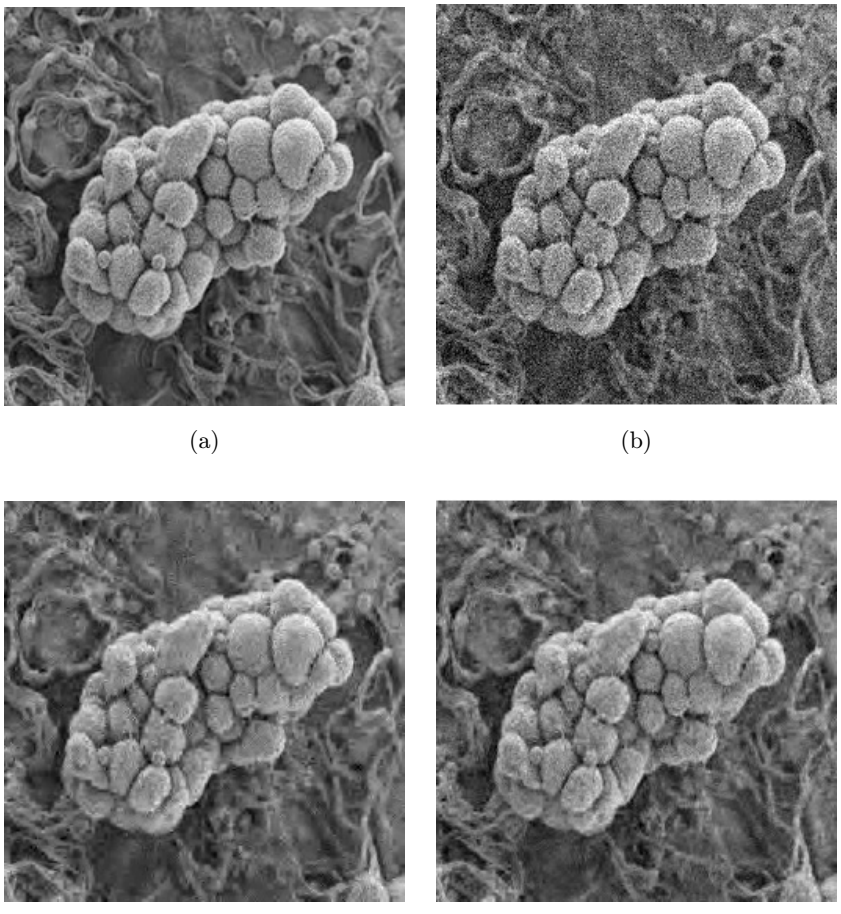

(a) (b) (c) (d)

Fig. 3. Comparison of denoising results of Cells image with $\sigma_n = 20$: (a) Noise-free, (b) Noisy image, (c) BayeShrink (PSNR = 27.24) and (d) Proposed method (PSNR = 27.59).

Moreover, in order for the processor in the proposed method (12) to be of any practical use, one should be able to estimate the noise-free variance σ^2 and noise variance σ_n^2 from the observed data. As proposed in Ref. 17, a robust estimate of the noise variance is obtained using the median absolute deviation of coefficients at the first level of an wavelet decomposition. For σ^2 estimation from noisy data have been previously proposed in Ref. 18.

3. Experimental Results

Here, experiments are carried out using three standard gray-scale images, namely, Barbara (512×512 pixels), Moon (256×256 pixels), and Cells (128×128 pixels). We use generalized incomplete gamma function for our proposed method. In fact, the first shrinkage function based on generalized incomplete gamma function is MLAP-MMSE.[13] So, we compared the proposed algorithm, bivariate case ($d = 2, \|\mathbf{y}\| = \sqrt{y_1^2 + y_2^2}$), using orthogonal discrete wavelet transform (DWT) to other effective systems in the literature, namely MLAP-MMSE and BayeShrink.[20] A six-level wavelet decomposition is carried out using Daubechies length-16 filter. In constant parameter K_2, $0.8 < K_2 < 1.3$ can also be a good choice. However, the experiments reveal that a $K_2 = 1$ provides the highest PSNR values in most cases. So, we report the results provided by our proposed denoising method using $K_2 = 1$. These algorithms are evaluated with different noise level $\sigma_n = 10, 15$, and 20. In local variance estimation of σ^2, 7×7 window size are used. In fact, we have not considered different windows size. The PSNR values are listed in Table 1. Each PSNR values in this table is averaged over 10 runs. In Table 1, the highest PSNR value is highlighted in bold letters. As we can seen from Table 1, the PSNR of our proposed method is better than conventional scheme. We compare the visual qualities of different denoising results, MLAP-MMSE and proposed method, of Barbara image, $\sigma_n = 10$, in Fig. 1. Figure 2 shows results from several denoising algorithms on Moon image with $\sigma_n = 15$, original image, noisy image, denoising image obtained from MLAP-MMSE, and our proposed method. Finally, we compare the visual qualities of different denoising results, BayeShrink and proposed method, of Cells image, $\sigma_n = 20$, in Fig. 3.

In fact, generalized incomplete gamma function is numerical function. So, some pixel of denoised image is not accurate. Here, we proposed average filter for this problem. MATLAB code of average filter can be found in Appendix C.

4. Conclusion and Discussion

In this paper, we present new MMSE estimator for GSM with Maxwell density in AWGN. In Bayesian techniques, instead of using MMSE estimator we can use the MAP estimator to obtain the denoising shrinkage function. Moreover, the results may be improved using more complex prior models e.g. mixture models. So, these assumptions are interesting questions.

Acknowledgments

Project supported by Institute of Research and Development Rajamangala University of Technology Ratanakosin, Thailand.

Appendix A. Generalized Incomplete Gamma Function

In Refs. 21 and 22, the generalized incomplete gamma function is defined as

$$\Gamma(\alpha, x; b) = \int_x^\infty t^{\alpha-1} \exp\left(-t - \frac{b}{t}\right) dt. \qquad \text{(A.1)}$$

For $\alpha = \pm 1/2$, the fundamental solutions are defined as[13,21,22]

$$\Gamma\left(\frac{1}{2}, x; b\right) = \begin{cases} 0.5\sqrt{\pi}\exp(-x) \\ \Big[\exp(x - 2\sqrt{b})\operatorname{erfc}(\sqrt{x} - \sqrt{b/x}) \\ +\exp(-b/x)\operatorname{erfcx}(\sqrt{x} + \sqrt{b/x})\Big], & x < 2\sqrt{b} \\ 0.5\sqrt{\pi}\exp(-x) \\ \Big[\exp(-b/x)\operatorname{erfcx}(\sqrt{x} - \sqrt{b/x}) \\ +\exp(-b/x)\operatorname{erfcx}(\sqrt{x} + \sqrt{b/x})\Big], & x > 2\sqrt{b}, \end{cases}$$

$$\Gamma\left(-\frac{1}{2}, x; b\right) = \frac{1}{\sqrt{b}}\Gamma\left(\frac{1}{2}, x; b\right),$$

where $\operatorname{erfcx}(x) := \exp(x^2)\operatorname{erfc}(x)$, $\operatorname{erfc}(x) := 1 - \operatorname{erf}(x)$, and $\operatorname{erf}(x) := \frac{2}{\sqrt{\pi}} \int_0^\infty \exp(-t^2) dt$. The recurrence

relation of generalized incomplete gamma function is[13,21,22]

$$\Gamma(\alpha-1,x;b) = \frac{1}{b}\left[\Gamma(\alpha+1,x;b)-\alpha\Gamma(\alpha,x;b) - x^{\alpha}\exp\left(-x-\frac{b}{x}\right)\right],$$

where $\alpha = -0.5, -1.5, -2.5, \ldots$. This solution is useful for computing its values for other orders α.

Appendix B. Gaussian Integration

In Ref. 23, if the random vectors $\mathbf{S}$ and $\mathbf{N}$ are zero-mean Gaussian with variance σ^2 and σ_n^2, respectively,

$$f_{\mathbf{S}}(\mathbf{s}) = \frac{1}{(2\pi\sigma^2)^{d/2}}\exp\left(\frac{-\|\mathbf{s}\|^2}{2\sigma^2}\right),$$
$$f_{\mathbf{N}}(\mathbf{n}) = \frac{1}{(2\pi\sigma_n^2)^{d/2}}\exp\left(\frac{-\|\mathbf{n}\|^2}{2\sigma_n^2}\right),$$

and $a > 0$, then,

$$\int_{\mathbb{R}^d}\frac{1}{a^d}f_{\mathbf{S}}\left(\frac{\mathbf{x}}{a}\right)f_{\mathbf{N}}(\mathbf{y}-\mathbf{x})d\mathbf{x} = \frac{1}{(2\pi(a^2\sigma^2+\sigma_n^2))^{d/2}}\exp\left(\frac{-\|\mathbf{y}\|^2}{2(a^2\sigma^2+\sigma_n^2)}\right), \tag{B.1}$$

$$\int_{\mathbb{R}^d}\frac{x_i}{a^d}f_{\mathbf{S}}\left(\frac{\mathbf{x}}{a}\right)f_{\mathbf{N}}(\mathbf{y}-\mathbf{x})d\mathbf{x} = \frac{y_i a^2\sigma^2}{(2\pi)^{d/2}(a^2\sigma^2+\sigma_n^2)^{\frac{d}{2}+1}}\exp\left(\frac{-\|\mathbf{y}\|^2}{2(a^2\sigma^2+\sigma_n^2)}\right). \tag{B.2}$$

Appendix C. The MATLAB Code of Average Filter

After inverse wavelet transform, in case we have 'nan' (not a number) or 'overflow' in denoised image 'z'. It is possible because the proposed algorithm is based on generalized incomplete gamma function, numerical function. We can use average filter algorithm. The MATLAB code of average filter is:

```
(1)  function z = average_pixel(z);
(2)  average_value = medfilt2(z, [17 17]);
(3)  Lower_bound = z < −20;
(4)  Upper_bound = z > 275;
(5)  NaN_value = isnan(z);
(6)  Inf_Value = isinf(z);
(7)  z = Lower_bound.*average_value...
(8)  + Upper_bound.*average_value...
(9)  + NaN_value.*average_value...
(10) + Inf_Value.*average_value...
(11) +(1 − (Lower_bound + Upper_bound +
     NaN_value + Inf_Value)).*z;
```

References

1. A. N. Pavlov, A. S. Abdurashitov, O. N. Pavlova, V. V. Tuchin, "Hidden stage of intracranial hemorrhage in newborn rats studied with laser speckle contrast imaging and wavelets," *J. Innov. Opt. Health Sci.* **8**, 1550041 (2015).
2. W. Gao, V. P. Zakharov, O. O. Myakinin, I. A. Bratchenko, D. N. Artemyev, D. V. Kornilin, "Medical images classification for skin cancer using quantitative image features with optical coherence tomography," *J. Innov. Opt. Health Sci.* **9**, 1650003 (2016).
3. A. S. Saad, G. A. El-Hiti, A. M. Masmali, "A computer-based image analysis for tear ferning featuring," *J. Innov. Opt. Health Sci.* **8**, 1550015 (2015).
4. H. C. Li, W. Hong., Y. R. Wu, P. Z. Fan, "Bayesian wavelet shrinkage with heterogeneity-adaptive threshold for SAR image despeckling based on generalized gamma distribution," *IEEE Trans. Geosci. Remote Sens.* **51**, 2388–2402 (2013).
5. S. M. M. Rahman, M. O. Ahmad, M. N. S. Swamy, "Bayesian wavelet-based image denoising using the Gauss-Hermite expansion," *IEEE Trans. Image Process.* **17**, 1755–1771 (2008).
6. F. Shi, I. W. Selesnick, "An elliptically contoured exponential mixture model for wavelet based image denoising," *Appl. Comput. Harmonic Anal.* **23**, 987–1017 (2007).
7. M. I. H. Bhuiyan, M. O. Ahmad, M. N. S. Swamy, "Wavelet-based image denoising with the normal inverse Gaussian prior and linear MMSE estimator," *IET Image Process.* **2**, 203–217 (2008).
8. H. Rabbani, M. Vafadust, P. Abolmaesumi, S. Gazor, "Speckle noise reduction of medical ultrasound images in complex wavelet domain using mixture priors," *IEEE Trans. Biomed. Eng.* **55**, 2152–2160 (2008).
9. A. Achim, P. Tsakalides, A. Bezerianos, "SAR image denoising via Bayesian wavelet shrinkage based on heavy-tailed modeling," *IEEE Trans. Geosci. Remote Sens.* **41**, 1773–1783 (2003).

10. J. Portilla, V. Strela, M. J. Wainwright, E. Simoncelli, "Image denoising using scale mixture of Gaussians in the wavelet domain," *IEEE Trans. Image Process.* **12**, 1338–1351 (2003).
11. P. A. Khazron, I. W. Selesnick, "Bayesian estimation of Bessel K form random vectors in AWGN," *IEEE Signal Process. Lett.* **15**, 261–264 (2008).
12. J. A. Guerrero, L. Mancera, J. Portilla, "Image restoration sparse-variant Gaussian scale mixtures in overcomplete pyramids," *IEEE Trans. Image Process.* **17**, 27–41 (2008).
13. I. W. Selesnick, "Laplace random vectors, Gaussian noise, and the generalized incomplete gamma function," *IEEE Int. Conf. Image Processing (ICIP)*, pp. 2097–2100, Atlanta, USA (2006).
14. F. Shi, I. W. Selesnick, "Multivariate quasi-Laplacian mixtures models for wavelet-based image denoising," *IEEE Int. Conf. Image Processing (ICIP)*, pp. 2625–2628, Atlanta, USA (2006).
15. S. G. Kim, Y. S. Kim, I. K. Eom, "Locally adaptive speckle noise reduction using maximum a posteriori estimation based on Maxwell distribution," *IEEE Int. Conf. Signal Processing Systems (SiPS)*, pp. 2625–2628, Tampere, France (2006).
16. H. M. Musal, "Logarithmic compression of Rayleigh and Maxwell distributions," *Proc. IEEE* **57**, 1311–1313 (1969).
17. D. L. Donoho, I. M. Johnstone, "Ideal spatial adaptation by wavelet shrinkage," *Biometrika* **81**, 425–455 (1994).
18. P. Kittisuwan, "MAP of Pearson type IV random vectors in AWGN," *IEEE Int. Conf. Electrical Engineering/Electronics, Computer, Telecommunications and Information Technology (ECTI-CON)*, pp. 1–4, Phetchaburi, Thailand (2012).
19. M. Abramowitz, I. A. Stegun, *Handbook of Mathematical Functions*, Dover Publications, New York (1964).
20. S. G. Chang, B. Yu, M. Vetterli, "Adaptive wavelet thresholding for image denoising and compression," *IEEE Trans. Image Process.* **9**, 1522–1531 (2000).
21. M. A. Chaudhry, S. M. Zubair, "Generalized incomplete gamma functions with applications," *J. Comput. Appl. Math* **55**, 99–124 (1994).
22. M. A. Chaudhry, S. M. Zubair, *On a Class of Incomplete Gamma Functions with Applications*, Chapman and Hall, New York (2001).